EVS24
Stavanger, Norway, May 13 - 16, 2009

Control-Oriented Dynamic Li-Ion Battery Models for High Power Applications

Ralf Bartholomaeus[1], Carsten Klaucke, Henning Wittig
Fraunhofer Institute for Transportation and Infrastructure Systems, Zeunerstrasse 38, 01069 Dresden, Germany
[1]*Corresponding author: ralf.bartholomaeus@ivi.fhg.de*

Abstract

In the design and development process of battery packs, single cell models are particularly important for tasks ranging from battery simulation up to model-based design of sophisticated battery management systems. In the literature a variety of modelling approaches have been proposed, which can be distinguished according to their resulting model structure and the method of model parameterization. The objective of the present work is to develop a systematic and efficient procedure for the coupled electric and thermal modelling of a lithium ion cell. The drawback of higher model complexity is compensated by a dedicated parameter estimation algorithm. Finally, the accuracy of the proposed model is shown by the comparison of simulation results with real measurements of a given cell.

Keywords: state of charge (SOC), battery model, lithium battery, parameter estimation

1 Introduction

Typically the design process of battery packs starts with a mathematical characterization of a single cell as it is the basic unit of the battery. The resulting model is then used for different tasks which include

A1: the simulation of the battery pack behaviour (e.g. non-uniformity in state-of-charge and the influence of contact resistances in a serial/parallel/matrix connected battery structure or the cooling power and coolant flow rate necessary to maintain proper thermal conditions),

A2: the design of diagnostic and monitoring systems (e.g. for real-time calculation of the state-of-charge, the state-of-health or the internal temperature of the cells), and

A3: the design of model-based energy management controllers and predictive cooling strategies for the battery pack.

For this aim, a macroscopic description of the coupled electrical and thermal behaviour of the battery cell turns out to be adequate. The inputs of that model are the electric current I and the cooling conditions characterized by the flow speed v and temperature ϑ_0 of the coolant. The overvoltage $\mathcal{U}$ and cell temperature ϑ are the state variables. The terminal voltage U, the electric charge $Q = \int I dt$ and a subvector of ϑ are the outputs. In general $\mathcal{U}$ and ϑ are vectors.

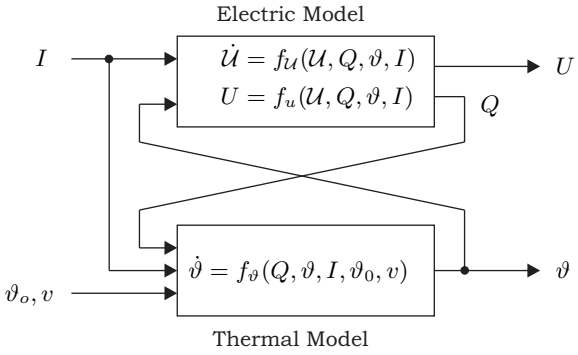

Figure 1: Battery model structure

Different approaches to the modelling of batteries have been proposed in the literature. Physics-based models [2, 1], presumably offering high

accuracy, are not suitable for commercial cells because they require detailed knowledge of internal processes and material properties that are often not available. Empirical models are offering a relatively low order and easier identification. Electro-impedance spectroscopy is often applied to obtain frequency domain data for the estimation of model parameters [4, 3]. Since this method assumes stationary conditions (i.e. Q and ϑ are nearly constant) during the experiments, it is difficult to identify large time constants. Moreover AC excitation has to be small compared to typical battery currents [3], so that for large currents I the model accuracy cannot be guaranteed. These drawbacks can be avoided by the use of models in the time domain, even though parameter estimation is numerically more complex for these models [5]. Another aspect regarding the achievable model accuracy is the incorporation of couplings between electrical and thermal behaviour of the cell.

2 Systematic modelling approach

In the following section the developed approach for the modelling of lithium ion cells is presented. A model structure is proposed that was formulated in order to obtain a precise simulation of system behaviour over a wide range of operational conditions. Interpretations of structural components and their dependence on different parameters like temperature and state of charge (SOC) are discussed. Furthermore it is shown that the proposed complex nonlinear model formulated in state space equations covers several other model approaches often reported in the literature.

Regarding operational conditions, high power applications put high demands on batteries. For instance, in hybrid electric vehicles, large power peaks (during acceleration and braking of the vehicle) as well as high energy transfer (when driving up and downhill) can occur. In these applications the current, the electric charge and the temperature of the battery undergo large variations and can reach the limits of the cells operational range. Therefore, the battery model is required to be valid in the whole feasible operational region.

To cover all relevant parameters and their dependencies, this paper proposes the model formulated in a state space representation according to equations (1a) and (1b).

$$\begin{aligned} x_i[k] = a_i\, x_i[k-1] + \\ \sum_{\mu=1}^{\bar{\mu}} \sum_{\nu=0}^{\bar{\nu}} \sum_{\kappa=0}^{\bar{\kappa}} b^{+}_{i,\mu,\nu,\kappa}\, I^{+}[k]^{\mu}\, Q[k]^{\nu}\, \vartheta[k]^{\kappa} \\ + \sum_{\mu=1}^{\bar{\mu}} \sum_{\nu=0}^{\bar{\nu}} \sum_{\kappa=0}^{\bar{\kappa}} b^{-}_{i,\mu,\nu,\kappa}\, I^{-}[k]^{\mu}\, Q[k]^{\nu}\, \vartheta[k]^{\kappa} \end{aligned} \tag{1a}$$

$$(i = 1, \ldots, n)$$

$$\begin{aligned} U[k] = \sum_{i=1}^{n} x_i[k] + \\ \sum_{\mu=0}^{\bar{\mu}} \sum_{\nu=0}^{\bar{\nu}} \sum_{\kappa=0}^{\bar{\kappa}} d^{+}_{\mu,\nu,\kappa}\, I^{+}[k]^{\mu}\, Q[k]^{\nu}\, \vartheta[k]^{\kappa} \\ + \sum_{\mu=0}^{\bar{\mu}} \sum_{\nu=0}^{\bar{\nu}} \sum_{\kappa=0}^{\bar{\kappa}} d^{-}_{\mu,\nu,\kappa}\, I^{-}[k]^{\mu}\, Q[k]^{\nu}\, \vartheta[k]^{\kappa} \end{aligned} \tag{1b}$$

The electrical behaviour of the battery can be classified by different components. The SOC, which can be estimated based on the open circuit voltage (OCV), is one of the most important parameter. Its static characteristic is described by the equation

$$OCV[k] = \sum_{\nu=0}^{n} d_{0,\nu,0}\, q[k]^{\nu}. \tag{2}$$

Furthermore the dependence on several operational parameters is modelled, including SOC and current direction. The latter can be illustrated by the data plotted in Fig. 2, which shows a sequence of current pulses, that were performed in different SOC regions and the resulting voltage profiles. The data was experimentally gathered from a high energy lithium ion cell, which was also used for parameter estimation in section 4. For a decreasing SOC an increasing overvoltage as well as an increasing asymmetry of charge and discharge behaviour can be seen. The model captures the illustrated effect by the input $Q[k]$ and the distinction of current by

$$\begin{aligned} I^{+}[k] &= \max\{0, I[k]\} \\ I^{-}[k] &= \min\{0, I[k]\}. \end{aligned}$$

Moreover the model structure comprises a nonlinear behaviour regarding the battery current. The existance of such a nonlinearity is shown in Fig. 3. During the cell test a current profile with pulses of different current rates but the same length were performed. Since the normalized voltage characteristics ΔU do not coincide there must be a nonlinear relation between current and terminal voltage.

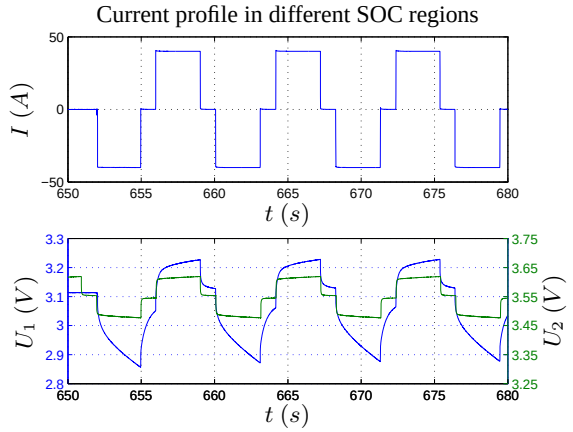

Figure 2: Results of cell tests analysing dependence of electrical behaviour on SOC

The proposed model (1a) and (1b) covers several other model approaches discussed in the literature.
A simplified model, as it is described in [9], is shown in Fig. 4. Unlike the proposed model it differentiate only between the series resistances R_c and R_d for charge and discharge respectively. Usually, the diffusion and double layer phenomena in the battery are realized by a distributed circuit model which consists of infinite RC ladder elements [4, 8] as shown in Figure 5. This series connected RC ladder circuit needs to be simplified. The determination of the number of elements n requires a trade-off between achievable model accuracy and processing power.

The proposed model also incorporates temperature dependent effects by introducing ϑ in the state-space representation. To avoid the costly measurement of temperatures, the thermal behaviour is modelled using the following equation

$$\vartheta[k+1] = a_{th}(\vartheta[k] - \vartheta_0) + b_{th} P_{th}[k] \ . \quad (3)$$

Herein ϑ denotes the cell's temperature, ϑ_0 the temperature of the coolant and P_{th} the generated thermal dissipation loss. For the model shown in Fig. 5 the thermal dissipation loss can be calculated utilizing the power loss of the resistances $R_0, \ldots, R_n$, thus obtaining

$$P_{th}[k] = I[k]^2 R_0 + \sum_{i=1}^{n} \frac{x_i[k]^2}{R_i} \ . \quad (4)$$

To determine the thermal dissipation loss for the model proposed in Eq. (1), the summations in Eq. (1a) are rearranged to

$$\underbrace{\left(\sum_{\mu=1}^{\bar{\mu}} \sum_{\nu=0}^{\bar{\nu}} \sum_{\kappa=0}^{\bar{\kappa}} b^{\pm}_{i,\mu,\nu,\kappa} \, I^{\pm}[k]^{\mu-1} \, Q[k]^{\nu} \, \vartheta[k]^{\kappa} \right)}_{:= b_i^{\pm}} \times I^{\pm}[k] \ .$$

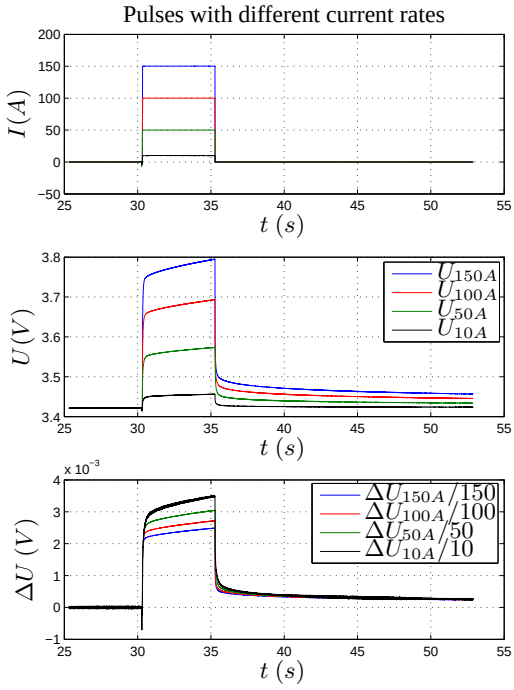

Figure 3: Results of cell tests analysing nonlinear behaviour regarding the current

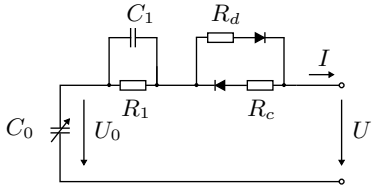

Figure 4: Simple equivalence model, R_c and R_d are the series resistances, R_1, C_1 describe diffusion and double layer phenomena

After transforming the model's discrete time parameters a_i and $b_i^{\pm}$ to continuous time parameters $\widetilde{a}_i$ and $\widetilde{b}_i^{\pm}$ respectively, the quotients $-\widetilde{b}_i^{\pm}/\widetilde{a}_i$ are equivalent to resistances $\widetilde{R}_i^{\pm}$, which are dependent on SOC, temperature and current. The resistances $\widetilde{R}_0^{\pm}$ are obtained in the same manner by rearranging Eq. (1b). Finally, the thermal dissipation loss for the nonlinear model can be calculated utilizing the power loss produced by $\widetilde{R}_0^{\pm}, \ldots, \widetilde{R}_n^{\pm}$.

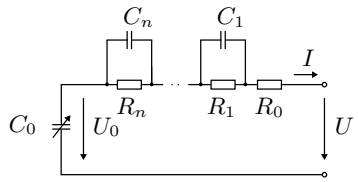

Figure 5: Simple equivalent circuit diagram of a battery. U and I are the terminal voltage and battery current, U_0 is the open circuit voltage, R_0 is the series resistance, R_1, C_1, ..., R_i, C_i describe diffusion and double layer phenomena

3 Parameter estimation with the SNLLS algorithm

In order to apply parameter estimation algorithms, the model introduced in Section 2 is usually written as $y = h(x, p)$, where the components of the vectors x and y are the time-discrete model inputs (I, ϑ_o and v) and model outputs (U and a subset of the components of ϑ) respectively. The vector p consists of the linear parameters $b_{i,\mu,\nu,\kappa}$, $d_{\mu,\nu,\kappa}$, $x_i[0]$ and the nonlinear parameters a_i. Parameter estimation is often done by fitting the model output $h(\tilde{x}, p)$ resulting from the input measurements $\tilde{x}$ to the output measurements $\tilde{y}$ in the least-squares sense. That means, p is determined by the solution of the problem

$$\|\tilde{y} - h(\tilde{x}, p)\|_2 \to \min_p . \tag{5}$$

Due to the large data sets emerging from experiments that cover a wide operational region (current rate, SOC, temperature) as well as a variety of battery characteristics with different time constants, the vectors $\tilde{x}$ and $\tilde{y}$ may consist of 10^5 to 10^8 components. Moreover the number of parameters can be large, e.g. defining the upper bounds of summations $\bar{\mu} = \bar{\nu} = \bar{\kappa} = 3$ already leads to a total number of parameters of $49n + 2n + 64$. Numerical solution of the resulting large-scale nonlinear estimation problems causes difficulties for standard least squares algorithms.
In order to apply more efficient methods, algorithms for separable nonlinear least-squares problems (SNLLS) [6] are adopted. The specific structure of the model is used to rewrite h in the separated form

$$y = F(x, \alpha, \beta) := \sum_{i=1}^{n} \alpha_i \, f_i(x, \beta),$$

where the vectors α and β represent the linear and the nonlinear parameters respectively. If β was known, then the optimal linear parameters $\alpha^*(\beta)$ could be obtained by simply solving a linear least-squares problem. Therefore, the problem (5) can be replaced by

$$\|\tilde{y} - F(\tilde{x}, \alpha^*(\beta), \beta)\| \to \min_\beta . \tag{6}$$

This leads to a significant decrease of the number of parameters. Referring to the above mentioned example the calculated number of parameters $49n + 2n + 64$ for Eq. 5 is reduced to n parameters $\beta = (a_1, \ldots, a_n)$ for the problem formulation in (6).
The reduction of the parameter space does not only decrease the processing power and memory requirements necessary to solve the parameter estimation problem. Moreover, no initial guesses are necessary for the linear parameters which improves the reliability of convergence. It has been shown that the algorithm converges in fewer iterations and is numerically more stable [6].
Within the SNLLS algorithm the matrix

$$\mathbf{\Phi}(\beta) = [f_1(\tilde{x}, \beta) \ldots f_m(\tilde{x}, \beta)]$$

and its Moore–Penrose generalized inverse $\mathbf{\Phi}^+(\beta)$ is defined. Using the functional

$$\alpha^*(\beta) = \mathbf{\Phi}^+(\beta)\tilde{y} \tag{7}$$

and the substitution

$$G(\beta) := (I - \mathbf{\Phi}(\beta)\mathbf{\Phi}^+(\beta))\tilde{y} \tag{8}$$

leads to the nonlinear optimization problem

$$\|G(\beta)\|_2 \to \min_\beta . \tag{9}$$

Gradient-based optimization methods for the solution of (10) require the Jacobian $G'(\beta)$ for the determination of a descent step direction. In order to avoid time-consuming numerical calculation of the Jacobian, an analytical form of $G'(\beta)$ is given in [6]. In that reference it is also discussed how a further increase in efficiency of the procedure can be obtained by using an approximated Jacobian (so-called Kaufman model) instead of $G'(\beta)$.

For the proposed model (1a) and (1b) it turned out that the initial value of β has significant influence on speed of convergence and quality of approximation. With the following sequential strategy an appropriate definition of initial values for β is provided in step (i).

PARAMETER ESTIMATION ALGORITHM FOR MODEL EQUATIONS (1a) AND (1b)

(i) Define mutually different time constants T_i $(i = 1, \ldots, r)$ by using a priori informations (e.g. preliminary tests). The T_i should cover the expected dynamic electrical behaviour of the battery. Using T_i determine

the initial values for the poles a_i of the discretized model

$$x_i[k] = a_i\, x_i[k-1] + b_i\, u[k] \quad (i = 1, \ldots, r)$$
$$y[k] = \sum_{i=1}^{n} x_i[k] + d\, u[k] + \\ + c_3\, q[k]^3 + c_2\, q[k]^2 + c_1\, q[k] + c_0 \tag{10}$$

and fit this model to the experimentally gathered data. Eliminate all multiple-order poles that can emerge from an overparameterization and form the vector $\beta = (\hat{a}_1, \ldots, \hat{a}_n)$ from the remaining poles $\hat{a}_i$.

(ii) Accomplish the parameter estimation algorithm for model equations (1a) and (1b) using the initial values $\beta = (\hat{a}_1, \ldots, \hat{a}_n)$.

Due to the reduced order of the model according to Eq. 10 depicted in Fig. 5, parameter estimation acquires less processing power compared to the model equations (1a) and (1b). The resulting initial values β provide a basis for optimizing the nonlinear model parameters in step (ii).

4 Application example

In this section, the practicability and the improved characteristics of the proposed approach will be illustrated by applying it to a 40Ah lithium ion planar cell as an example of a cell which is designed for use in traction batteries. During cell tests only moderate current rates where used that caused no significant change in temperature. Hence temperature is modelled as a constant input variable $\vartheta = const.$ and the model equations (1a) and (1b) are simplified as follows

$$x_i[k] = a_i\, x_i[k-1] + \sum_{\mu=1}^{\bar{\mu}} \sum_{\nu=0}^{\bar{\nu}} b_{i,\mu,\nu}\, u[k]^\mu\, q[k]^\nu$$
$$(i = 1, \ldots, n)$$
$$y[k] = \sum_{i=1}^{n} x_i[k] + \sum_{\mu=0}^{\bar{\mu}} \sum_{\nu=0}^{\bar{\nu}} d_{\mu,\nu}\, u[k]^\mu\, q[k]^\nu. \tag{11}$$

To cover a wide range of operational regions, the performed cell tests comprise a sequence of constant-current pulses and rests with different length in random order within a SOC region of nearly 100%.

The models to be compared are the following

- Model A: resulting from step (i) of the algorithm in section 3
- Model B: according to Eq. (11), where the nonlinear parameters a_i are equal to those of model A and the linear parameters are optimized according to Eq. (7)
- Model C: according to Eq. (11), where the nonlinear parameters a_i are optimized according to step (ii) of the algorithm in section 3 and the linear parameters are optimized using Eq. (7)

Table 1: Simulation results

	n=1	n=4
Model A		
$T_{c,i}$ (s)	685	28,117,1574,7746
$\|G(\beta)\|_2$ (mV)	5.65	4.80
ΔU (mV)	7.20	6.05
Model B		
$\|G(\beta)\|_2$ (mV)	3.46	1.43
ΔU (mV)	4.45	1.89
Model C		
$T_{c,i}$ (s)	575	28, 120, 1556, 8179
$\|G(\beta)\|_2$ (mV)	3.43	1.42
ΔU (mV)	4.51	1.88

Table 1 summarizes the results of parameter estimation for the models A, B and C. Using the poles a_i the related time constants for the continuous-time model representation are calculated with the sample time T_s by

$$T_{C,i} = \frac{T_s}{-\ln a_i}. \tag{12}$$

The model performance is evaluated by the value of the target function (9) as well as the mean deviation ΔU between measured terminal voltage and the model output. Between model A and B a significant performance jump can be seen. Furthermore time constants in model A are already close to their optimal values, indicated by the value of target function (9) that is not improved as much.
Comparing models A and C (Fig. 6), performance of model C is improved especially at the boundary of the SOC region. Fig. 7 shows the model error of both models for the entire data set.

5 Conclusion

This paper presents a procedure that is practical for the modelling of lithium ion cells. The usage of a complex coupled electrical and thermal model allows for a high accuracy. By introducing the SNLLS algorithm, which is applied to parameterize the reduced electrical model in the previous section, it is possible to deal with large measurement data sets as well as a large number of parameters in an efficient way. The proposed methods are a promising approach for the extraction of battery models with a high accuracy in an extended operational region.

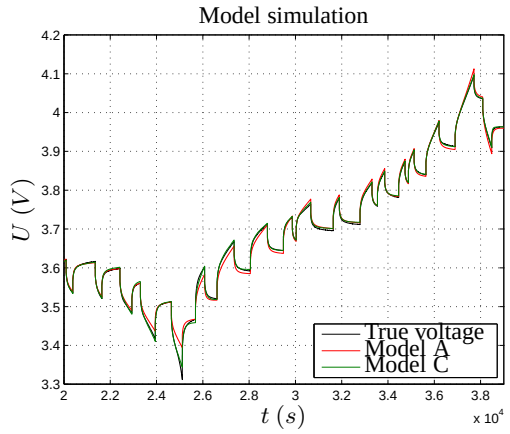

Figure 6: Results of cell modelling using models A and C

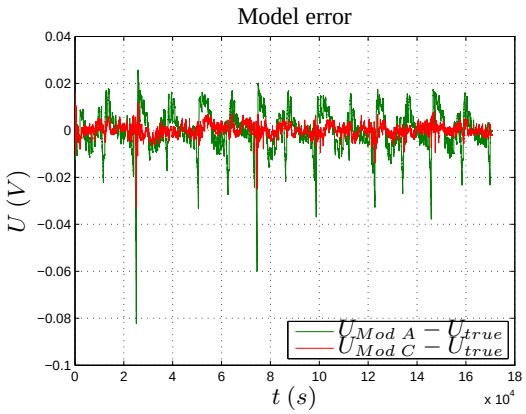

Figure 7: Deviation between terminal voltage and model output of model A and C

References

[1] Kandler A. Smith, Chao-Yang Wang, *Power and thermal characterization of a lithium-ion battery pack for hybrid-electric vehicles*, Journal of Power Sources, ISSN 0378-7753, 160(2006), 662-673.

[2] Kandler A. Smith, Christopher D. Rahn, Chao-Yang Wang, *Control oriented 1D electrochemical model of lithium ion battery*, Energy Conversion and Management, ISSN 0196-8904, 48(2007), 2565-2578.

[3] Eckhard Karden, Stephan Buller, Rik W. De Doncker, *A method for measurement and interpretation of impedance spectra for industrial batteries*, Journal of Power Sources, ISSN 0378-7753, 85(2000), 72-78.

[4] Stephan Buller, Marc Thele, Rik W. De Doncker, Eckhard Karden, *Impedance-Based Simulation Models of Supercapacitors and Li-Ion Batteries for Power Electronic Applications*, IEEE Transactions on Industry Applications, ISSN: 0093-9994, 41(2005), 742-747.

[5] Min Chen, Gabriel A. Rincon-Mora, *Accurate Electrical Battery Model Capable of Predicting Runtime and I-V Performance*, IEEE Transactions on Energy Conversion, ISSN: 0885-8969, 21(2006), 504-511.

[6] G.H. Golub, V. Pereyra, *The differentiation of pseudoinverses and nonlinear least squares problems whose variables separate*, SIAM Journal on Numerical Analysis, ISSN: 0036-1429, 10(1973), 413-432.

[7] Lijun Gao, Shengyi Liu, Roger A. Dougal, *Dynamic Lithium-Ion Battery Model for System Simulation*, IEEE Transactions on Components and Packaging Technologies, ISSN: 1521-3331, 25(2002), 495-505.

[8] Bernhard Schweighofer, Klaus M. Raab, Georg Brasseur, *Modeling of High Power Automotive Batteries by the Use of an Automated Test System*, IEEE Transactions On Instrumentation And Measurement, ISSN: 0018-9456, 52(2003), 1087-1091.

[9] Jaemoon Lee, Oanyong Nam, B.H. Cho, *Li-ion battery SOC estimation method based on the reduced order extended Kalman filtering*, Journal of Power Sources, ISSN 0378-7753, 174(2007), 9-15.

Authors

R. Bartholomaeus studied Control Engineering and Mathematics. In 1993 he joined the Fraunhofer Institute for Transportation and Infrastructure Systems (IVI) as a Research Associate. His research activities are mainly in the area of modelling and control of hybrid-electric power trains.

C. Klaucke studied Electrical Engineering (Automation and Control) at Technische Universität Dresden, Dresden, Germany.
Since November 2007, he has been a Research Associate with the Fraunhofer Institute for Transportation and Infrastructure Systems (IVI), Dresden, Germany. His research activities are in the area of modelling and simulation of energy storage systems.

H. Wittig studied Electrical Engineering (Automation and Control) at Technische Universität Dresden, Dresden, Germany.
Since November 2007, he has been a Research Associate with the Fraunhofer Institute for Transportation and Infrastructure Systems (IVI), Dresden, Germany. His research activities are in the area of modelling and simulation of energy storage systems.